

# Engineering of a Protein with Cyclooxygenase and Prostacyclin Synthase Activities That Converts Arachidonic Acid to Prostacyclin<sup>†</sup>

Ke-He Ruan,\* Hui Deng, and Shui-Ping So

Vascular Biology Research Center and Division of Hematology, Department of Internal Medicine, The University of Texas Health Science Center, Houston, Texas 77030

Received July 14, 2006; Revised Manuscript Received August 24, 2006

**ABSTRACT:** Prostacyclin (PGI<sub>2</sub>), a vascular protector with vasodilation and antithrombotic properties, is synthesized by coupling reactions of cyclooxygenase (COX, the first enzyme) with PGI<sub>2</sub> synthase (PGIS, the second enzyme) using arachidonic acid (AA) as an initial substrate. The first COX product, prostaglandin H<sub>2</sub> (PGH<sub>2</sub>) is also a common substrate for other prostanoid enzymes that produce distinct eicosanoids, such as thromboxane A<sub>2</sub> (TXA<sub>2</sub>). The actions of TXA<sub>2</sub> to cause vasoconstriction and platelet aggregation oppose the vasodilatory and anti-aggregatory effects of PGI<sub>2</sub>. Specifically upregulating PGI<sub>2</sub> biosynthesis is an ideal model for the prevention and treatment of the TXA<sub>2</sub>-mediated thrombosis involved in strokes and myocardial infarctions. Here, we report that a single protein was constructed by linking COX-2 and PGIS together to form a new fusion enzyme through a transmembrane domain with 10 or 22 residues. The engineered protein expressed in HEK293 and COS-7 cells was able to continually convert AA to prostaglandin (PG) G<sub>2</sub> (catalytic step 1), PGH<sub>2</sub> (catalytic step 2), and PGI<sub>2</sub> (catalytic step 3). The studies first demonstrate that a single protein with three catalytic functions could directly synthesize PGI<sub>2</sub> from AA with a *K<sub>m</sub>* of approximately 3.2 μM. Specific upregulation of PGI<sub>2</sub> biosynthesis through expression of the engineered single protein in the cells has shown strong activity in inhibiting platelet aggregation induced by AA *in vitro*, which creates a great potential for the fusion enzyme to be used as one of the new therapeutic interventions for strokes and heart attacks. The studies have also provided a model linking COX with its downstream enzymes to specifically regulate biosynthesis of eicosanoids which have potent biological functions.

The recent discovery that cyclooxygenase (COX)<sup>1</sup> isoform-2 (COX-2) inhibitors may be linked to heart disease has greatly increased the interest in understanding the biology of COX enzymes, which convert a lipid molecule, arachidonic acid (AA) into different prostanoids (part of the eicosanoid family) having diverse and/or opposite biological functions. Figure 1A outlines the biosynthesis of prostanoids, comprising of prostaglandins and thromboxane, formed via the COX pathway from AA in three catalytic (tricyclic) steps (1–3) by COX and its downstream synthases: AA released from the membrane phosphoglycerides is converted to the prostaglandin G<sub>2</sub> (PGG<sub>2</sub>, catalytic step 1), and then to prostaglandin endoperoxide (prostaglandin H<sub>2</sub> (PGH<sub>2</sub>)) (catalytic step 2) by COX isoform-1 (COX-1) or COX-2. PGH<sub>2</sub> is further isomerized to the biologically active end-products of prostaglandin D<sub>2</sub> (PGD<sub>2</sub>), E<sub>2</sub> (PGE<sub>2</sub>), F<sub>2</sub> (PGF<sub>2</sub>), and I<sub>2</sub> [PGI<sub>2</sub> (prostacyclin)] or thromboxane A<sub>2</sub> (TXA<sub>2</sub>) by individual synthases (catalytic step 3) in tissue-specific processes.

Prostanoids act as local hormones in the vicinity of their production site to regulate hemostasis and smooth muscle functions. Unlike the stable expression of COX-1, COX-2 expression is inducible and responds to the stimuli by pro-inflammatory and other pathogenic factors (6). TXA<sub>2</sub> produced from PGH<sub>2</sub> by TXA<sub>2</sub> synthase (TXAS) has been implicated as a proaggregatory and vasoconstricting mediator in various pathophysiological conditions (7, 8). PGI<sub>2</sub> is the primary AA metabolite in vascular walls and has opposing biological properties than TXA<sub>2</sub> and therefore represents the most potent endogenous vascular protector acting as an inhibitor of platelet aggregation (9) and a strong vasodilator on vascular beds (10–13). PGE<sub>2</sub> exhibits a variety of biological activities in inflammation. Aspirin and nonsteroidal anti-inflammatory drugs (NSAID) inhibit both COX-1 and COX-2 activities to reduce the production of all prostanoids, which leads to the thinning of blood by reducing TXA<sub>2</sub> production and the suppression of inflammation by decreasing PGE<sub>2</sub> production. The selective COX-2 inhibiting drugs exhibit anti-inflammatory effects similar to aspirin and NSAIDs, but they also may promote strokes and heart attacks by decreasing the production of PGI<sub>2</sub> and increasing the production of TXA<sub>2</sub>. When the COX-2 enzyme is inactivated by COX-2 inhibitors, the PGH<sub>2</sub> produced by COX-1 is still available for converting into other prostanoids, such as TXA<sub>2</sub> by TXAS, leading to an increased risk of thrombosis and vasoconstriction (6).

<sup>†</sup> This work was supported by NIH Grants (RO1 HL56712 and HL79389 for K.-H.R.).

\* To whom correspondence should be addressed: Division of Hematology, Department of Internal Medicine, University of Texas Health Science Center at Houston, 6431 Fannin St., Houston, Texas 77030. Tel.: 713-500-6769. Fax: 713-500-6810. E-mail: Ke.H.Ruan@uth.tmc.edu.

<sup>1</sup> Abbreviations: PCR, polymerase chain reaction; AA, arachidonic acid; HPLC, high-performance liquid chromatography; BSA, bovine serum albumin.

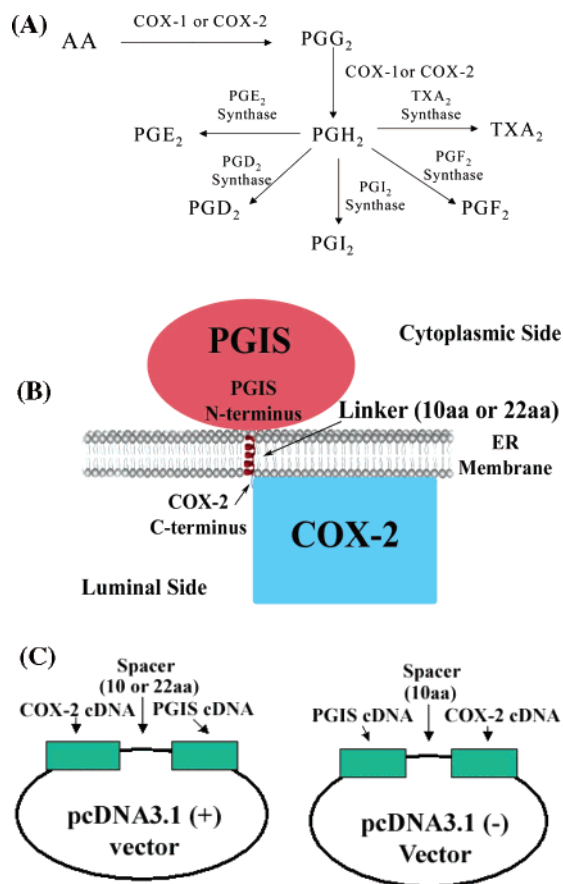


FIGURE 1: (A) Biosynthesis of prostanoids through the coordination of COXs and their downstream synthases. (B) Putative model of the coordination between COX-2 and PGIS in the ER membrane. COX-2 and PGIS proteins are located in the ER luminal and cytoplasmic sides anchored to the ER membrane, respectively. The engineered COX-2-linker-PGIS linked the two proteins together through a transmembrane domain with 10 or 22 amino acid residues without alteration of the protein topologies are shown. (C) Engineered cDNA plasmids containing COX-2 and PGIS protein sequences. COX-2 linked to PGIS, and PGIS linked to COX-2 through the 10aa or 22aa sequence were generated by a PCR approach and subcloning procedures provided by the vector company (Invitrogen). Briefly, the corresponding cDNA sequences were isolated from the pSG5 vector containing human COX-2 or PGIS by PCR using the primers containing the 10aa or 22aa with KpnI or Bam HI cutting sites at both ends (the 5' end of the anti-sense primer was connected with the DNA sequences of the designed linker). The resultant cDNA segments were cut with the corresponding restriction enzymes and subcloned into the corresponding sites at the pcDNA 3.1 vector.

A selective increase in the production of PGI<sub>2</sub> with a decrease in both TXA<sub>2</sub> and PGE<sub>2</sub> productions is the ideal model for (i) preventing and protecting against vascular diseases including inflammation, thrombosis, atherosclerosis, strokes and heart attacks, and (ii) benefiting the reproductive processes (14–16). From aspirin to the more recently developed COX-2 inhibitors, the drugs have not yet achieved this goal. Finding a way to specifically increase the production of the vascular protector, PGI<sub>2</sub>, will be one of the most attractive drug developments in pharmaceutical intervention. In this paper, we describe an innovative engineering of a recombinant protein with triple catalytic activities directly converting AA into PGI<sub>2</sub>, an important vascular protector. The successful engineering of the protein has provided evidence that COX enzymes could be linked with their downstream enzymes to specifically regulate the biosynthesis

of eicosanoids which play important roles in inflammation and vascular functions.

## EXPERIMENTAL PROCEDURES

**Materials.** COS-7 and HEK293 cell lines were purchased from ATCC (Manassas, VA). Medium for culturing the cell lines was purchased from Invitrogen. [<sup>14</sup>C]AA was purchased from Amersham. Goat anti-rabbit IgG-FITC conjugate, saponin, streptolysin O, Triton X-100, and triethylenediamine were purchased from Sigma (St. Louis, MO). Mowiol 4-88 was purchased from Calbiochem (San Diego, CA).

**Cell Culture.** COS-7 or HEK293 cells were cultured in a 100-mm cell culture dish with high glucose Dulbecco's modified Eagle's medium containing 10% fetal bovine serum and antibiotic and antimycotic, and were grown at 37 °C in a humidified 5% CO<sub>2</sub> incubator.

**Engineered cDNA Plasmids with Single Genes Encoding the COX-2 or PGIS Sequences.** The cDNAs of the engineered COX-2-10aa-PGIS, COX-2-22aa-PGIS, and PGIS-10aa-COX-2 were successfully cloned into the pcDNA 3.1 vector containing a cytomegalovirus early promoter using a polymerase chain reaction (PCR) cloning approach (Figure 1C). The correct sequences were confirmed by DNA sequencing and endonuclease digestion analyses. COX-2 linked to PGIS and PGIS linked to COX-2 through the 10aa or 22aa sequences were generated by a PCR approach and subcloning procedures provided by the vector company (Invitrogen). Briefly, the corresponding cDNA sequences were isolated from the pSG5 vector containing human COX-2 or PGIS by PCR using the primers containing the DNA encoding:

For 10aa (COX-2 sense: cgggtaccatgctcgcgcgcctg; COX-2-10aa antisense: cgggtacccaggtgaaggcgacgccatgatggcgtgcagttcagtcgaacgttcttttag); for 22aa (COX-2-22aa antisense: cgggtaccgacagtggtgcccgcgcacaggccagaccatgacccaggtgaaggcgacgcc atgatggcgtgcagttcagtcgaacgttcttttag) with KpnI or Bam HI cutting sites at both ends (the 5' end of the anti-sense primer was connected with the DNA sequences of the designed linker). The resulted cDNA segment was cut with the corresponding restriction enzymes and ligated into the corresponding sites of the pcDNA 3.1 vector. The cDNA sequences of the molecules were confirmed by restriction enzyme digestion and further identified by DNA sequencing.

**Expression of the Synthases in COS-7 or HEK293 Cells.** The recombinant synthases were expressed in COS-7 or HEK293 cells as described (17–18). Briefly, the cells were grown and transfected with a purified cDNA of the recombinant protein by the Lipofectamine 2000 method (19) following the manufacturer's instructions (Invitrogen). Approximately 48 h after transfection, the cells were harvested for further enzyme assay and a Western blot was performed. For the cotransfection, a 3:2 ratio of cDNAs of COX-2 and PGIS were used for the transfection.

**Preparation of Microsomal Fractions of COS-7 or HEK293 Cells and Western Blot.** The general procedure for microsome preparation was previously described (20). The transfected or untransfected COS-7 cells were scraped from the plates into ice-cold PBS buffer, pH 7.4, and collected by centrifugation. After the cells were washed three times, the pellet was resuspended in a small volume of the same buffer, sonicated briefly, and centrifuged at 10000g for 10

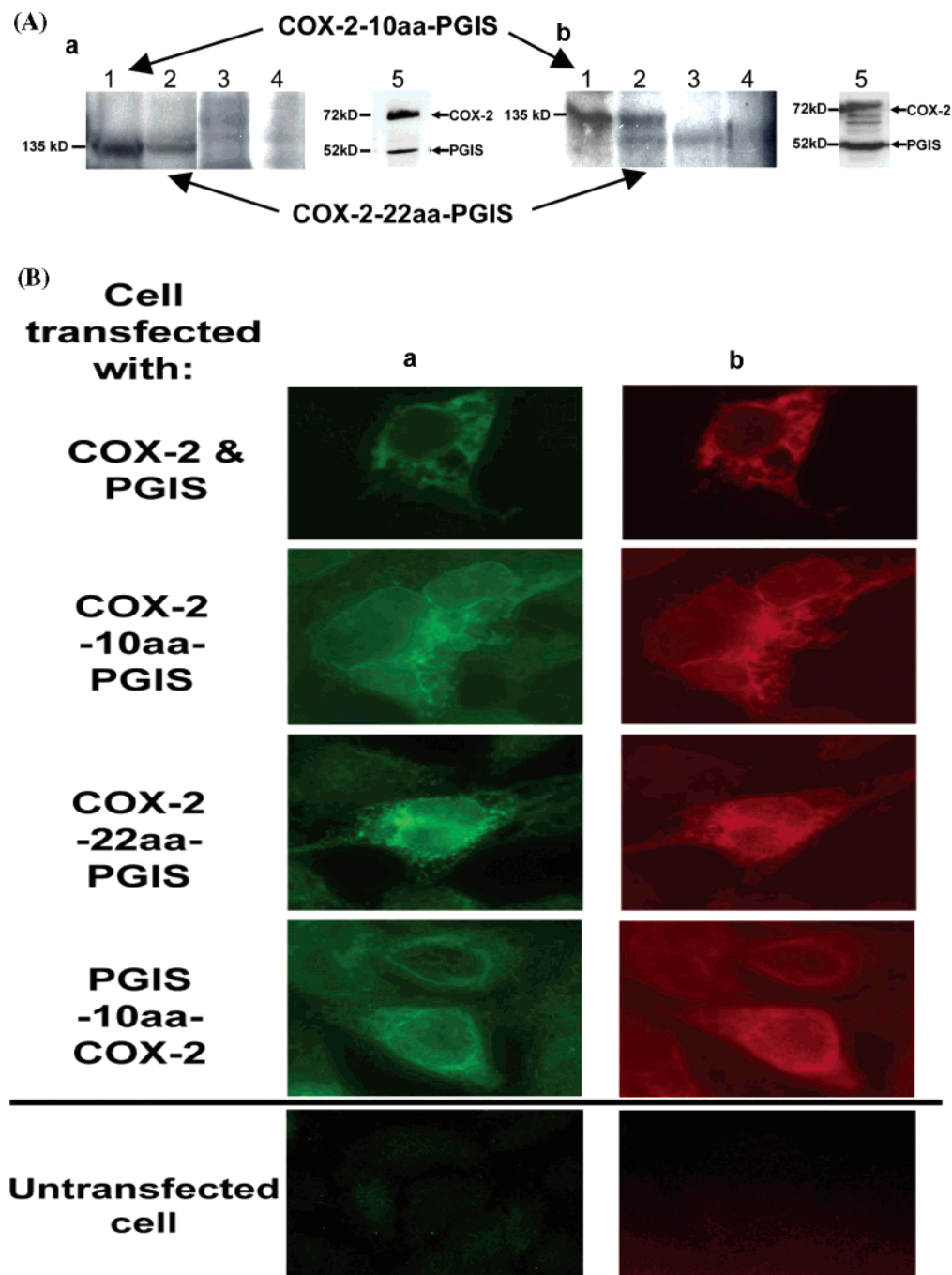


**FIGURE 2:** (A) Western blot analysis of the overexpressed recombinant proteins in COS-7 (a) or HEK293 (b) cells. The procedures were described previously (21–22, 24). Briefly, COS-7 or HEK293 cells were grown for 24 h to 90–95% confluent and then transfected with the purified cDNA plasmid [24  $\mu$ g/dish (100 mm)] by the Lipofectamine 2000 method (19) following the manufacturer's instructions (Invitrogen). For the cotransfection, the cells were transfected with 12  $\mu$ g of human COX-2 cDNA plasmid and 8  $\mu$ g of human PGIS cDNA plasmid. Approximately 48 h after transfection, the cells were harvested for Western blot analysis. A total of 20  $\mu$ g of the proteins of the cells transfected with the cDNA(s) [COX-2-10aa-PGIS (lane 1), COX-2-22aa-PGIS (lane 2), PGIS-10aa-COX-2 (lane 3), or untransfected cells (lane 4)] was subjected to 7% SDS-PAGE and then transferred onto a nitrocellulose membrane. The cells cotransfected with COX-2 and PGIS in HEK cells (panel a, lane 5) and COS-7 cells (panel b, lane 5) were also analyzed by the same method. All of the membranes were probed with rabbit anti-PGIS peptide antibody and anti-COX-2 peptide antibody and then stained with horseradish peroxidase-labeled goat-anti rabbit antibody. The numbers on the left side represent the molecular weight of the engineered fusion enzyme, COX-2, and PGIS which are indicated with arrows. (B) Immunofluorescence micrographs of HEK293 cells. The general procedures for the indirect immunostaining were described previously (23–24, 27). In brief, the cells were grown on cover-slides and transfected with the cDNA plasmid(s) as described in panel A. The cells were generally permeabilized by saponin and then incubated with the affinity-purified rabbit anti-PGIS peptide antibody (a) and mouse anti-COX-2 antibody (b) (24). The bound antibodies were stained by FITC-labeled goat-anti rabbit IgG (a) or rhodamine-labeled goat anti-mouse IgG (b). The stained cells were examined by fluorescence microscopy (24).

min. The supernatant was collected and centrifuged at 200000g for 40 min to pellet the microsomal fraction (20). The recovery of the microsomal protein from one of the dish cells was 0.2–0.3 mg. Microsomal proteins were separated

by 10% (w/v) PAGE under denaturing conditions and then transferred to a nitrocellulose membrane. Bands recognized by particular primary antibodies were visualized with horseradish peroxidase-conjugated secondary antibody and

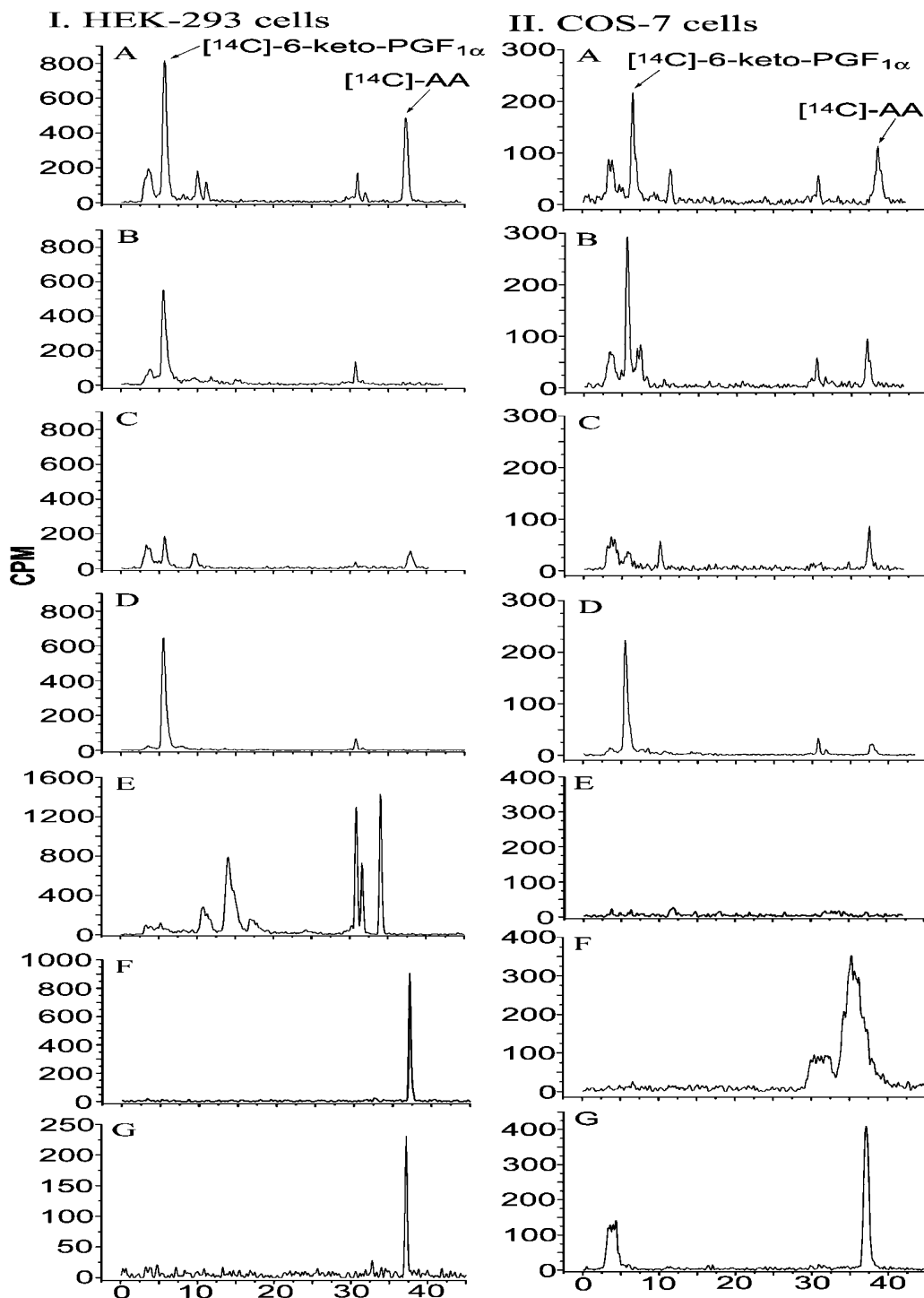


FIGURE 3: Determination of the tricatalytic activities of the recombinant proteins directly converting AA to PGI<sub>2</sub> using an HPLC method for HEK293 cells (panel I) and COS-7 cells (panel II). The cells ( $\sim 0.1 \times 10^6$ ) transfected with the recombinant cDNA(s) of COX-2-22aa-PGIS (A), COX-2-10aa-PGIS (B), PGIS-10aa-COX-2 (C), COX-2 and PGIS (D), COX-2 alone (E) or PGIS alone (F) (as described in Figure 2A) or the untransfected cells (G) were washed three times, suspended in 0.01 M phosphate buffer, pH 7.4 containing 0.15% NaCl (PBS) and then incubated with [<sup>14</sup>C]-AA (10  $\mu$ M) in a total volume of 30  $\mu$ L. After 5 min, the reaction was terminated by the addition of 50  $\mu$ L of 0.1% acetic acid containing 35% acetonitrile (buffer A), and centrifuged at 12 000 rpm for 5 min. The supernatant was separated by HPLC on a C18 column (4.5  $\times$  250 mm) using buffer A with a gradient of 35–100% acetonitrile. The [<sup>14</sup>C]-AA metabolites were determined by a liquid scintillation analyzer built in the HPLC system. The retention times of [<sup>14</sup>C]-6-keto-PGF<sub>1α</sub> and [<sup>14</sup>C]-AA were calibrated by standards under the same conditions. The amounts of produced 6-keto-PGF<sub>1α</sub> represented the amounts of the produced PGI<sub>2</sub>.

chromogenic peroxidase substrates (20). Normalization of the PGIS and TXAS in microsomal and detergent-solubilized proteins was based on the intensities of the bands in the immunoblot.

**Enzyme Activity Determination for COX and PGIS Using the HPLC Method.** To determine the activities of the

synthases that converted AA to PGI<sub>2</sub> through the tricatalytic functions, different concentrations of [<sup>14</sup>C]-AA (0.3–60  $\mu$ M) were added to the mixture in a total volume of 30  $\mu$ L. After 0.5–5 min of incubation, the reaction was stopped by adding 50  $\mu$ L of the solvent containing 0.1% acetic acid and 30% acetonitrile (solvent A). After centrifugation (12 000 rpm for



5 min), the supernatant was injected into a C18 column (Varian Microsorb-MV 100-5,  $4.6 \times 250$  mm) using the solvent A with a gradient from 35 to 100% of acetonitrile for 45 min at a flow-rate of 1.0 mL/min. The [ $^{14}$ C]-labeled AA metabolites, including 6-keto-PGF $_{1\alpha}$  (degraded PGI $_2$ ) were monitored directly by a flow scintillation analyzer (Packard 150TR).

**Enzyme Activity Determination for COX and PGIS Using Enzyme Immunoassay (EIA).** The supernatant of the reaction mixture as described above was diluted 100 times using PBS containing 0.1% bovine serum albumin and then used for determination of the end-product, 6-keto-PGF $_{1\alpha}$  (degraded PGI $_2$ ) using an EIA kit following the manufacturer's instructions (Cayman).

**Immunofluorescence Staining.** Transfected cells grown on a cover glass were washed with PBS and then incubated with 1% saponin for 20 min. The cells were then incubated with the primary antibody (10  $\mu$ g/mL of affinity-purified anti-human COX-2 or PGIS antibody) in the presence of 0.25% saponin for 1 h. After washing using PBS, the cells were incubated with the secondary antibodies (20). Cells stained with the FITC- or rhodamine-labeled antibody were viewed under the Zeiss Axioplan 2 epifluorescence microscope.

**Anti-Platelet Aggregation Assays.** A sample of fresh blood was collected using a collection tube with 3.2% sodium citrate for anticoagulation. A total of 300  $\mu$ L of this blood was combined with 300  $\mu$ L of saline solution and placed inside the 37 °C incubator of a whole blood anticoagulation analyzer (DYNABYTE; Germany) for a total of 3 min. Meanwhile, non-transfected HEK293 cells as well as those transfected with the recombinant cDNAs of COX-2-10aa-PGIS or COX-2 coexpressed with PGIS were incubated with 2.7 mM arachidonic acid for 30 s. The cells were then separately injected into the blood/saline mixtures inside the platelet aggregometer's incubator and readings were obtained indicating the amount of platelet aggregation produced by each of the treated samples. These data were collected by the anticoagulation analyzer and translated into more comparable information using the ORIGIN 6.1 program.

## RESULTS

**Design of a Recombinant Protein with Triple Catalytic Activities Directly Converting Arachidonic Acid into Prostaglandin.** Recent studies of the structural and functional relationship of COX enzymes and PGIS have advanced our knowledge of the molecular mechanisms involved in the biosynthesis of PGI $_2$  in native cells. Crystallographic studies of detergent-solubilized COX-1 and COX-2 suggest that the catalytic domains of the proteins lie on the luminal side of the endoplasmic reticulum (ER) and are anchored to the ER membrane by the hydrophobic side chains of the amphipathic helices A–D. These hydrophobic side chains of the putative membrane anchor domains also form an entrance to the substrate-binding channel and potentially form an initial docking site for the lipid substrate, AA (21–22). Our recent progress in the topological and structural studies of human PGIS and TXAS has led to the proposal of models in which PGIS and TXAS have catalytic domains on the cytoplasmic side of the ER, opposite the orientation of COXs (23–26). In this configuration, the substrate channels of all three enzymes, COX, PGIS, and TXAS, open at or near the ER

membrane surface. This suggests that the coordination between COXs and PGIS or TXAS in the biosynthesis of TXA $_2$  and PGI $_2$  is facilitated by the anchoring of the enzyme in the ER membrane (26). These studies have indicated that the physical distances between COXs and PGIS are very small. It led us to hypothesize that it is possible to create a single protein molecule containing COX and PGIS sequences with minimum alteration of both enzymes' folding and membrane topologies by extending the N-terminal membrane anchor domain of PGIS using a transmembrane sequence linked to the COX-1 or COX-2, which then adopts the functions of both enzymes of COX and PGIS (Figure 1B). In this case, AA can be directly converted into the vascular protector, PGI $_2$ , and thus, it decreases the productions of unwanted PGE $_2$  and TXA $_2$ . To test this hypothesis, a linker with 10 (His-Ala-Ile-Met-Gly-Val-Ala-Phe-Thr-Trp (10aa)) or 22 (His-Ala-Ile-Met-Gly-Val-Ala-Phe-Thr-Trp-Val-Met-Ala-Leu-Ala-Cys-Ala-Ala-Pro-Pro-Leu-Val (22aa)) residues of the structurally defined helical transmembrane domain of bovine rhodopsin were used to configure the engineered cDNA containing the COX-2 and PGIS sequences. The sequence begins at the N-terminus of COX-2, which is linked to either 10aa (COX-2-10aa-PGIS) or 22AA (COX-2-22AA-PGIS), and then linked to the N-terminus of PGIS that ends with the C-terminus of PGIS (Figure 1C). In contrast, an engineered cDNA containing reversed order from PGIS to 10aa to COX-2 was also prepared as a control (PGIS-10aa-COX-2) (Figure 1C). The reason COX-2 was selected for the preparation of the fusion enzyme is based on the assumption that COX-2 may favor coupling with PGIS more so than COX-1 would in the biosynthesis of PGI $_2$ .

**Expression of the Engineered Recombinant Protein in COS-7 and HEK Cell Lines.** The expression of the recombinant proteins was tested in a COS-7 cell line (monkey epithelial cells) and an HEK293 cell line (human embryonic kidney 293 cells) by a transient protein expression approach using LipofectamineTM2000 (Invitrogen). COX-2-10aa-PGIS and COX-2-22aa-PGIS were successfully overexpressed in both cell lines by showing a molecular weight of approximately 130 kDa in Western blot analysis (Figure 2A). In contrast, the expressed PGIS-10aa-COX-2 protein was undetectable by Western blot (Figure 2A) indicating that it may have been degraded due to the lack of a correct protein folding. Positive controls showing the coexpressed COX-2 and PGIS proteins in HEK and COS-7 cells with similar levels to that of COX-2-22aa-PGIS and COX-2-10aa-PGIS are also shown (Figure 2A). To test whether the expressed COX-2-10aa-PGIS and COX-2-22aa-PGIS can anchor to the ER membrane and adopt similar membrane topologies as the native COX-2 and PGIS enzymes, fluorescence immunostaining was used to localize the subcellular distribution of the engineered enzymes overexpressed in COS-7 cells. Similar staining patterns were observed in the COS-7 cells expressing the engineered proteins and the cells coexpressing the individual COX-2 and PGIS enzymes when stained with either anti-human PGIS (Figure 2B, panel a) or anti-human COX-2 (Figure 2B, panel b) antibodies. This could be described as a perinuclear pattern of distribution of immunocytofluorescence that is consistent with a location in membranes contiguous with the nuclear membrane, such as the ER membrane. In contrast, a low-level expression of protein was detected in the cells transfected with the PGIS-

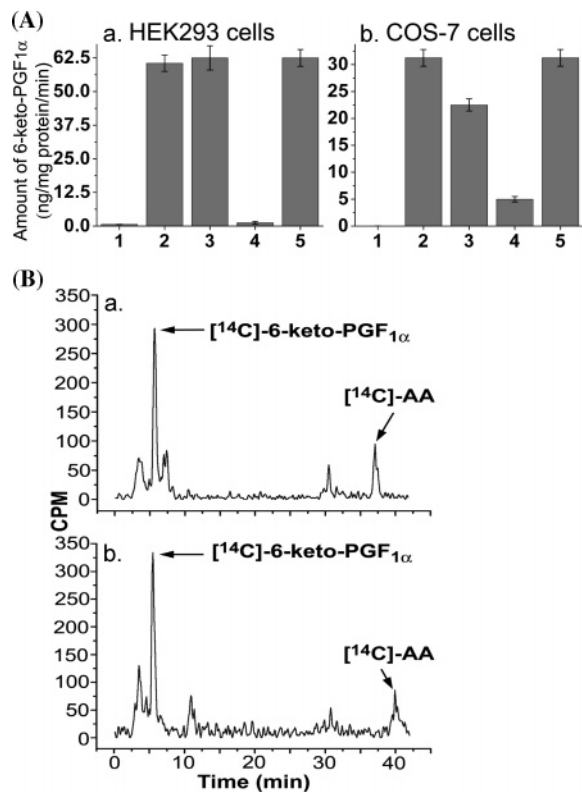


FIGURE 4: (A) Determination of the tricatlytic activities of the recombinant proteins directly converting AA to PGI<sub>2</sub> using enzyme immunoassay (EIA). After the enzyme reactions as described in Figure 3, the reaction mixtures (1. Untransfected cells, 2. COX-2-22aa-PGIS, 3. COX-2-10aa-PGIS, 4. PGIS-10aa-COX-2, and 5. coexpressed COX-2 and PGIS) were diluted 100 times with PBS containing 0.1% BSA, and then used for quantitative determination of 6-keto-PGF<sub>1α</sub> using an EIA kit following the instructions of the manufacturer (Cayman Chemical, Ann Arbor, MI). (B) Comparison of the tricatlytic activities of the engineered COX-2-10aa-PGIS in the cells and in the membrane preparation. The tricatlytic activities of COX-2-10aa-PGIS expressed in COS-7 cells were determined using the intact cells (a) as described in Figure 3. The same amount of the cells was homogenized and the total membrane protein collected from ultracentrifugation was used for the activity assay (b). The amounts of 6-keto-PGF<sub>1α</sub> represented the amounts of the produced PGI<sub>2</sub>.

10aa-COX-2 cDNA (Figure 2B) indicating that the engineered COX-2-10aa-PGIS and COX-2-22aa-PGIS have similar ER membrane anchoring functions as the native COX-2 and PGIS enzymes, and higher expression levels than that of PGIS-10aa-COX-2.

**Directly Converting Arachidonic Acid into the Vascular Protector, Prostacyclin by the Engineered Protein with Triple Catalytic Activities.** Evidence for the conversion of AA into the vascular protector, PGI<sub>2</sub> (by the tricatlytic reactions in a single protein of COX-2-10aa-PGIS or COX-2-22aa-PGIS) was given by two independent assays: high performance liquid chromatography (HPLC) analysis (Figure 3) and enzyme immunoassay (EIA, Figure 4A), using AA as a substrate for the cells overexpressing the engineered proteins. The tricatlytic activities in the engineered single protein were identical to the reactions mediated by two enzyme proteins of COX-2 and PGIS coexpressed in the cells (Figures 3 and 4A). It shall be noted that the synthesized PGI<sub>2</sub> was unstable and quickly degraded into the more stable 6-keto-PGF<sub>1α</sub>. Thus, the level of 6-keto-PGF<sub>1α</sub> shown in the HPLC and EIA represent the amounts of PGI<sub>2</sub> produced by

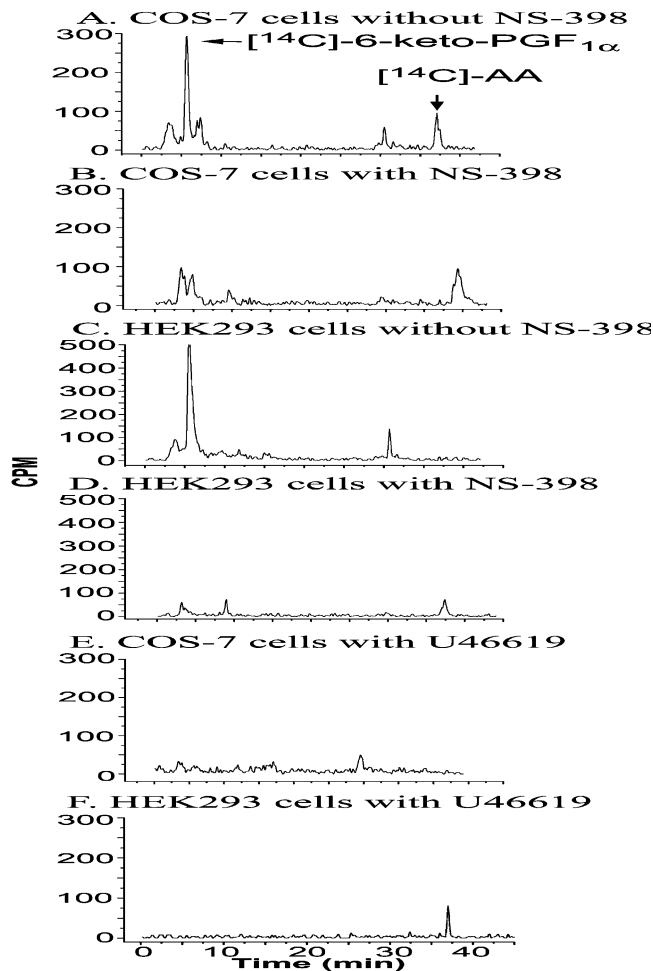


FIGURE 5: The effects of the COX-2 inhibitor on the tricatlytic activities of COX-2-10aa-PGIS. The conversion of AA to PGI<sub>2</sub> by the COX-2-10aa-PGIS overexpressed in COS-7 (A, B, and E) and in HEK293 (C, D, and F) cells were compared in the absence (A and C) and presence (B and D) of a COX-2 inhibitor, NS-398 (60 μM), or in the presence (E and F) of a PGIS inhibitor, U46619 (60 μM), using an HPLC method as described in Figure 3.

the enzymatic reactions (Figures 3 and 4A). COX-2-10aa-PGIS and COX-2-22aa-PGIS expressed in the intact cells exhibited very similar tricatlytic activities in the direct conversion of AA to PGI<sub>2</sub>. Similar catalytic activities were also observed for the membrane protein preparations as well as the intact cells (Figure 4B). Thus, the COX-2-10aa-PGIS was used as an example for further studies involving enzymatic properties. The biological activity of the overexpressed COX-2-10aa-PGIS in HEK293 cells and COS-7 cells which directly converted [14C]-AA to [14C]-PGI<sub>2</sub> was further confirmed by two inhibition assays using a COX-2 inhibitor, NS-398 and a PGIS inhibitor, U46619 (Figure 5; 26). The dramatically reduced PGI<sub>2</sub> production caused by the addition of NS-398 or U46619 indicated that the PGI<sub>2</sub> production from AA was specifically catalyzed by the COX-2-linker-PGIS protein (Figure 5).

**Kinetic Studies for Directly Converting Arachidonic Acid into Prostacyclin by the Engineered Protein with Triple Catalytic Activities.** Kinetic studies have clearly revealed that both COX-2-10aa-PGIS and COX-2-22aa-PGIS have *K<sub>m</sub>* values (~3.2–3.5 μM, Figure 6A) very similar to the reported *K<sub>m</sub>* values for the individual COX-2 and PGIS enzymes. These data demonstrate that the engineered COX-2-linker-PGIS is able to adopt the wild types of COX-2 and

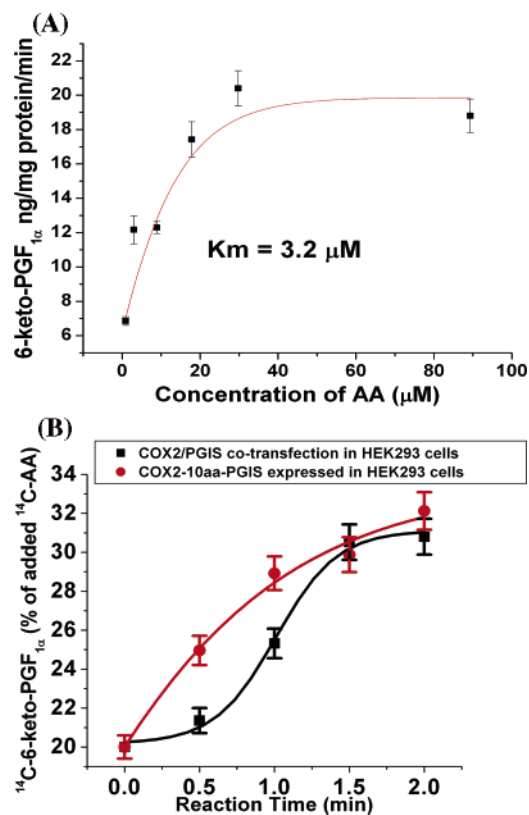


FIGURE 6: (A) Enzyme kinetic properties of the COX-2-10aa-PGIS with the tricatalytic activities. Different concentrations of AA were added to the membrane preparations of the COS-7 cells overexpressing the COX-2-10aa-PGIS protein ( $\sim 20 \mu\text{g}$ ). After an incubation period of 5 min, the degraded  $\text{PGI}_2$  product, 6-keto- $\text{PGF}_{1\alpha}$ , was determined by the EIA method as described in Figure 4A. The membrane preparation of the untransfected COS-7 cells was used as a control. Each point is the average of three individual assays. ( $n = 3$ ). (B) Time-course of the conversion of AA to  $\text{PGI}_2$  by the recombinant proteins. The conversion of AA to  $\text{PGI}_2$  by the COX-2-10aa-PGIS (●) or the coexpressed COX-2 and PGIS in the HEK293 cells (■) was performed with different reaction times using the EIA method as described in Figure 4A. The amounts of the produced  $\text{PGI}_2$  (6-keto- $\text{PGF}_{1\alpha}$ ) at different reaction times were plotted. The untransfected cells were used as controls.

PGIS activities. The tricatalytic activities involved in converting AA to  $\text{PGG}_2$  and ultimately to  $\text{PGH}_2$  and  $\text{PGI}_2$  can be completed by the COX-2-linker-PGIS protein. Additionally, in time course studies, the tricatalytic turnover activities of the COX-2-10aa-PGIS in the first 0.5–1 min reaction was faster than the reactions using the two enzymes of COX-2 and PGIS coexpressed in the cells (Figure 6B). This provides strong evidence in which the engineered protein molecules show a promising capability to compete with the endogenous COX-downstream synthases to convert COX-generated  $\text{PGH}_2$  to  $\text{PGI}_2$ . Thus, the engineered COX-2-linker-PGIS not only adopts both the COX and the PGIS activities but may also increase the selectivity to convert AA to  $\text{PGI}_2$ . This is particularly important in pathophysiological conditions, in which the quick conversion of AA or  $\text{PGH}_2$  to  $\text{PGI}_2$  will reduce the substrate available to other COX-downstream synthase pathways such as TXAS and PGES. It will lead to a decrease in the biosynthesis of  $\text{TXA}_2$  and  $\text{PGE}_2$  in the cells. An anti-platelet aggregation assay was used to show the vascular protective function of the engineered protein. When the membrane fraction of the cells overexpressing the COX-2-10aa-PGIS protein was added to the fresh blood, the AA-

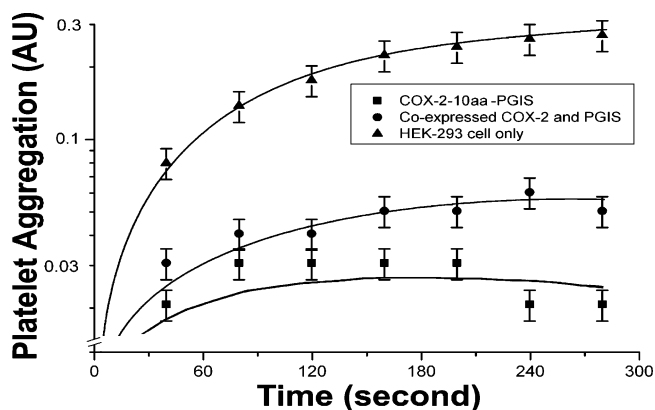


FIGURE 7: Inhibitory activity of  $\text{PGI}_2$  generated by the COX-2-linker-PGIS protein on platelet aggregation in vitro. Fresh blood was drawn and kept in an anticoagulant solution. A total of 300  $\mu\text{L}$  of blood and 300  $\mu\text{L}$  saline were mixed and incubated at  $37^\circ\text{C}$  for 3 min. During incubation, 20  $\mu\text{L}$  of the HEK293 cells (▲) transfected with the recombinant cDNA of COX-2-10aa-PGIS (■) or that of the COX-2 coexpressed with PGIS (●) were treated as described in Figure 3 and incubated with 2.7 mM AA for 30 s. The cells were then injected into the blood sample and the platelet aggregation signals were transferred to the computer and plotted.

stimulated platelet aggregation was dramatically inhibited (Figure 7). Furthermore, it was noted that the inhibition capacity resulting from the COX-2-10aa-PGIS was much stronger and longer-lasting than the addition of a mixture of the membrane fractions of the cells overexpressing COX-2 and PGIS proteins (Figure 7). In contrast, the membrane fraction of the cells transfected with the vector alone did not show any inhibition (Figure 7). The results indicate that the engineered protein was able to produce  $\text{PGI}_2$  instantly in the whole blood environment against the platelet aggregation and have more selectivity and capacity to produce  $\text{PGI}_2$  than the mixture of COX-2 and PGIS. This is important for preventing and reversing thrombosis, hypertension, and ischemic tissues resulting from  $\text{TXA}_2$  and for the reduction of vascular inflammation stimulated by  $\text{PGE}_2$ . The cDNA of the COX-2-linker-PGIS can potentially be used as a gene therapy reagent to prevent and treat thrombosis associated with strokes and heart attacks. More specifically, the biologically active COX-2-linker-PGIS protein can be used as a reagent by injection into tissues to instantly synthesize  $\text{PGI}_2$  against thrombosis in vivo.

## DISCUSSION

The advantages of the newly engineered COX-2-linker-PGIS protein can be highlighted as follows: (1) The protein design has demonstrated that multiple catalytic enzyme activities can be configured within a single protein molecule if an approximate protein configuration is adopted. (2) The studies show evidence that suggests the engineered protein with tricatalytic functions not only accumulates the individual enzymes' activities but also has a faster turnover rate when compared to the mixture of the parent enzymes. (3) It is known that COX-1 shares similar molecular features with COX-2 rendering the method used for preparation of COX-2-linker-PGIS suitable for general preparation of the COX-1-linker-PGIS molecule. (4) The two enzyme functions of COX-2 and PGIS combined into one protein molecule imply that the same design can be used to make single molecules



containing COX-1 or COX-2 linked with their downstream synthases, such as COX-linker-PGES, COX-linker-PGDS, and COX-linker-PGFS.

The success of the COX-2-linker-PGIS engineering also helps to understand several important controversies in COX biology: (1) The concept that the enzymatic activities of COXs occur under the conditions of the defined dimerization structures has been generally adopted because the studies of crystal structures for detergent-solubilized COX-1 and COX-2 revealed that the active enzymes were in dimer forms. This concept is not fully supported by current studies because it is highly probable that the engineered protein has different dimerization features relative to the native COX enzymes. (2) The exact physical distances between COXs and their downstream synthases in the cells during the biosynthesis of prostanoids were unknown. Current studies clearly demonstrate that the distance between the two enzymes must be very close because the turnover rate of the isomerization of PGH<sub>2</sub> to PGI<sub>2</sub> in the cells coexpressed with COX-2 and PGIS has a more limited delay than the single molecule of COX-2-10aa-PGIS, which has an approximate 10 Å separation between the catalytic sites of COX-2 and PGIS (Figure 6B).

Currently in gene therapy, introducing the COX gene alone into cells may not increase the biosynthesis of PGI<sub>2</sub> due to the limited amount of endogenous PGIS in the cells. Introducing the PGIS gene alone into the cell also may not be able to increase PGI<sub>2</sub> synthesis due to the limited amount of endogenous COXs in the cells. Co-introducing COX and PGIS genes into cells could increase the difficulty of gene delivery and may not control the specific PGI<sub>2</sub> production due to the competition of other downstream synthases, which share PGH<sub>2</sub> as their substrate. For example, it is especially difficult to avoid the overproduction of PGE<sub>2</sub> by tissue injuries during gene delivery using viral vectors (27). The engineered COX-2-linker-PGIS eliminates the step of PGH<sub>2</sub> movement from the COX protein to the PGIS protein in the different locations leading to increased PGI<sub>2</sub> production and limiting PGH<sub>2</sub> availability for TXA<sub>2</sub> and PGE<sub>2</sub> production. Thus, it can be a new generation of cDNA for COX gene therapy. On the other hand, the COX-linker-PGIS protein can be developed into a therapeutic reagent to instantly increase PGI<sub>2</sub> production locally via injection. It is particularly interesting that COX-2 inhibitors inhibit COX-2 activity but not the COX-1 activity; thus, introduction of the COX-1-linker-PGIS to cardiovascular systems can potentially overcome the side effects of the COX-2 inhibitors that cause damage to cardiovascular functions. In conclusion, given the importance of PGI<sub>2</sub> in vascular diseases and thrombosis, the engineered COX-linker-PGIS will be a useful molecule for in vivo studies in developing therapeutic interventions.

## ACKNOWLEDGMENT

We thank Dr. Richard J. Kulmacz and Lee-Ho Wang for providing the original wild type cDNAs of human COX-2 and PGIS, respectively. We also thank Dr. Miguel Escobar for assisting in the anti-platelet aggregation assays. In addition, we thank NIH for supporting this work under grant numbers of HL56712 and HL79389 (for K.-H. Ruan), and Brandi Hobratschk and Vanessa Cervantes for the assistance of the manuscript preparation.

## REFERENCES

1. Majerus, P. W. (1983) Arachidonate metabolism in vascular disorders, *J. Clin. Invest.* 72, 1521–1525.
2. Pace-Asciak, C. R., and Smith, W. L. (1983) Enzymes in the biosynthesis and catabolism of the eicosanoids: prostaglandins, thromboxanes, leukotrienes and hydroxy fatty acids, *Enzymes* 16, 544–604.
3. Samuelson, B., Goldyne, M., Granstrom, E., Hamberg, M., Hammarstrom, S., and Malmsten, C. (1978) Prostaglandins and thromboxanes, *Ann. Rev. Biochem.* 47, 994–1030.
4. Smith, W. L. (1986) Prostaglandin biosynthesis and its compartmentation in vascular smooth muscle and endothelial cells, *Ann. Rev. Physiol.* 48, 251–262.
5. Funk, C. D. (2001) Prostaglandins and leukotrienes: advances in eicosanoid biology, *Science* 294, 1871–1875.
6. Vane, J. R. (2002) Biomedicine. Back to an aspirin a day? *Science* 296, 474–475.
7. Needleman, P., Turk, J., Jackschik, B. A., Morrison, A. R., and Lefkowitz, J. B. (1986) Arachidonic acid metabolism, *Annu. Rev. Biochem.* 55, 69–102.
8. Bunting, S., Gryglewski, R., Moncada, S., and Vane, J. R. (1976) Arterial walls generate from prostaglandin endoperoxides a substance (prostaglandin X) which relaxes strips of mesenteric and coeliac arteries and inhibits platelet aggregation, *Prostaglandins* 12, 897–913.
9. Moncada, S., Herman, A. G., Higgs, E. A., and Vane, J. R. (1977) Differential formation of prostacyclin (PGX or PGI<sub>2</sub>) by layers of the arterial wall. An explanation for the anti-thrombotic properties of vascular endothelium, *Thromb. Res.* 11, 323–344.
10. Weksler, B. B., Ley, C. W., and Jaffe, E. A. (1978) Stimulation of endothelial cell prostacyclin production by thrombin, trypsin, and the ionophore A 23187, *J. Clin. Invest.* 62, 923–930.
11. Ingberman-Wojenski, C., Silver, M. J., Smith, J. B., and Macarak, E. (1981) Bovine endothelial cells in culture produce thromboxane as well as prostacyclin, *J. Clin. Invest.* 67, 1292–1296.
12. Smith, W. L., DeWitt, D. L., and Allen, M. L. (1983) Biomedical distribution of the prostaglandin I<sub>2</sub> synthesis antigen in smooth muscle cells, *J. Biol. Chem.* 258, 5922–5926.
13. Jakobsson, P. J., Thoren, S., Morgenstem, R., and Samuelsson, B. (1999) Identification of human prostaglandin E synthase: a microsomal, glutathione-dependent, inducible enzyme, constituting a potential novel drug target, *Proc. Natl. Acad. Sci. U.S.A.* 96, 7220–7225.
14. Huang, J. C., Goldsby, J. S., Arbab, F., Melhem, Z., Aleksic, N., and Wu, K. K. (2004) Oviduct prostacyclin functions as a paracrine factor to augment the development of embryos, *Hum. Reprod.* 19, 2907–2912.
15. Huang, J. C., Goldsby, J. S., and Wun, W. S. (2004) Prostacyclin enhances the implantation and live birth potentials of mouse embryos, *Hum. Reprod.* 19, 1856–1860.
16. Huang, J. C., Wun, W. S., Goldsby, J. S., Wun, I. C., Falconi, S. M., and Wu, K. K. (2003) Prostacyclin enhances embryo hatching but not sperm motility, *Hum. Reprod.* 18, 2582–2589.
17. Deng, H., Wu, J., So, S. P., and Ruan, K. H. (2003) Identification of the residues in the helix F/G loop important to catalytic function of membrane-bound prostacyclin synthase, *Biochemistry* 42, 5609–5617.
18. Ruan, K. H., Deng, H., Wu, J., and So, S. P. (2005) The N-terminal membrane domain of the membrane-bound prostacyclin synthase involved in the substrate presentation in the coupling reaction with cyclooxygenase, *Arch. Biochem. Biophys.* 435, 372–381.
19. Hatae, N., Yamaoka, K., Sugimoto, Y., Negishi, M., and Ichikawa, A. (2002) Augmentation of receptor-mediated adenylyl cyclase activity by Gi-coupled prostaglandin receptor subtype EP3 in a Gbetagamma subunit-independent manner, *Biochem. Biophys. Res. Commun.* 290, 162–168.
20. Lin, Y. Z., Deng, H., and Ruan, K. H. (2000) Topology of catalytic portion of prostaglandin I(2) synthase: identification by molecular modeling-guided site-specific antibodies, *Arch. Biochem. Biophys.* 379, 188–197.
21. Picot, D., Loll, P. J., and Garavito, R. M. (1994) The X-ray crystal structure of the membrane protein prostaglandin H2 synthase-1, *Nature* 367, 243–249.
22. Luong, C., Miller, A., Barnett, J., Chow, J., Ramesha, C., and Browner, M. F. (1996) Flexibility of the NSAID binding site in the structure of human cyclooxygenase-2, *Nat. Struct. Biol.* 3, 927–933.



23. Deng, H., Huang, A., So, S. P., Lin, Y. Z., and Ruan, K. H. (2002) Substrate access channel topology in membrane-bound prostacyclin synthase, *Biochem. J.* 362, 545–551.
24. Ruan, K. H., So, S. P., Zheng, W., Wu, J., Li, D., and Kung, J. (2002) Solution structure and topology of the N-terminal membrane anchor domain of a microsomal cytochrome P450: prostaglandin I<sub>2</sub> synthase, *Biochem. J.* 368, 721–728.
25. Wu, J., So, S. P., and Ruan, K. H. (2003) Determination of the membrane contact residues and solution structure of the helix F/G loop of prostaglandin I<sub>2</sub> synthase, *Arch. Biochem. Biophys.* 411, 27–35.
26. Ruan, K. H. (2004) Advance in understanding the biosynthesis of prostacyclin and thromboxane A<sub>2</sub> in the endoplasmic reticulum membrane via the cyclooxygenase pathway, *Mini Rev. Med. Chem.* 4, 639–647.
27. Hirschowitz, E., Hidalgo, G., and Doherty, D. (2002) Induction of cyclo-oxygenase-2 in non-small cell lung cancer cells by infection with DeltaE1, DeltaE3 recombinant adenovirus vectors, *Gene Ther.* 9, 81–84.

BI0614277